BMC Plant Biology

RESEARCH Open Access

# Genome-wide identification of the grapevine β-1,3-glucanase gene (*VviBG*) family and expression analysis under different stresses

Ling Wang[1,2*], Ruilong Li[1,2], Kaiwei Li[1,2], Ziyang Qu[3], Ruijin Zhou[1,2], Guilong Lu[1,2], Peng Li[1,2] and Guirong Li[1,2*]

## Abstract

**Background** The β-1,3-glucanase gene is widely involved in plant development and stress defense. However, an identification and expression analysis of the grape β-1,3-glucanase gene (*VviBG*) family had not been conducted prior to this study.

**Results** Here, 42 *VviBGs* were identified in grapevine, all of which contain a GH-17 domain and a variable C-terminal domain. *VviBGs* were divided into three clades α, β and γ, and six subgroups A–F, with relatively conserved motifs/domains and intron/exon structures within each subgroup. The *VviBG* gene family contained four tandem repeat gene clusters. There were intra-species synteny relationships between two pairs of *VviBGs* and inter-species synteny relationships between 20 pairs of *VviBGs* and *AtBGs*. The *VviBG* promoter contained many *cis*-acting elements related to stress and hormone responses. Tissue-specific analysis showed that *VviBGs* exhibited distinct spatial and temporal expression patterns. Transcriptome analysis indicated that many *VviBGs* were induced by wounds, UV, downy mildew, cold, salt and drought, especially eight *VviBGs* in subgroup A of the γ clade. RT-qPCR analysis showed that these eight *VviBGs* were induced under abiotic stress (except for *VviBG41* under cold stress), and most of them were induced at higher expression levels by PEG6000 and NaCl than under cold treatment.

**Conclusions** The chromosome localization, synteny and phylogenetic analysis of the *VviBG* members were first conducted. The *cis*-acting elements, transcriptome data and RT-qPCR analysis showed that *VviBG* genes play a crucial role in grape growth and stress (hormone, biotic and abiotic) responses. Our study laid a foundation for understanding their functions in grape resistance to different stresses.

**Keywords** Grapevine, β-1,3-glucanase gene family, Abiotic stress, Expression pattern

*Correspondence:
Ling Wang
wangling@hist.edu.cn
Guirong Li
ligrapes@hist.edu.cn
[1]College of Horticulture and Landscape Architecture, Henan Institute of Science and Technology, Xinxiang 453003, China
[2]Henan Province Engineering Research Centers of Horticultural Plant Resource Utilization and Germplasm Enhancement, Xinxiang 453003, China
[3]State Key Laboratory of Crop Genetics and Germplasm Enhancement, College of Resources and Environmental Sciences, Nanjing Agricultural University, Nanjing 210095, China

## Background

Callose, or β-1,3-glucan, is a 1,3-β-D-linked glucose homopolymer, which is a polysaccharide found only in embryophytes. The regulation of plasmodesmata (PD) conductivity by callose is a dynamic process, and the accumulation of callose in the neck of PD is strictly controlled by the antagonistic effects of two enzymes, namely callose synthase (CalS) and β-1,3-glucanase (BG), which respectively confer synthesis and degradation of β-1,3-glucan [1].

BG acts as a hydrolase, catalyzing the intramolecular cleavage of 1,3-β-D-glucosidic bonds into individual β-1,3-glucan units. To date, a complex and diverse *BG* gene family has been found in tobacco [2], soybean [3], Arabidopsis [4], rice [5] and cotton [6]. Plant BGs are classified into three structural classes: class I vacuolar proteins [7], class II and class III acidic secreted proteins [8], and unique intercellular "ersatz" BGs contained within class I [9]. In Arabidopsis, there are 50 AtBGs, all of which contain an N-terminal signal peptide and a glycosyl hydrolase family 17 (GH-17) domain, with some also containing a C-terminal domain X8 (also known as CBM43) [4]. A recent study identified 67 (*Gossypium. raimondii*), 68 (*G. arboretum*), 130 (*G. hirsutum* acc. TM-1) and 158 (*G. barbadense* acc. 3–79) β-1,3-glucanase genes (*GLUs*) in four cotton species, and found that *GLU42* and *GLU43* positively regulate cotton resistance to *Verticillium dahliae* [6].

BGs are commonly referred to as pathogenesis-related (PR) proteins, primarily acting by directly degrading pathogen cell walls [10]. *Pyrus pyrifolia* gene *PpGlu* enhances tobacco resistance to several pathogenic fungi [11]. *Ah-Glu* gene enhances peanut resistance to fungal pathogen *Cercospora personifita* [12]. *TcLr19Glu* participates in the defense response of wheat against rust pathogens [13]. Wheat β-1,3-glucanase exerts inhibitory effects on fungi associated with wheat grains [14]. *PnGlu1* gene from *Panax notoginseng* confers resistance in tobacco to *Fusarium solani* [15]. *Gns6* is an important effector in the defense response of rice against pathogenic fungi [16]. Plant growth promoting bacteria induce the formation of a complex between the β-1,3-glucanase gene and GTP in host plants, resulting in resistance to rice blast fungus [17]. β-1,3-GLU2 is involved in the main defense response of mango against *C. gloeosporioides*, and SNP 21,881,933 enhances the activity of β-1,3-glucanase [18]. *SlBG10* regulates tomato pollen, fruit and seed development and disease resistance by regulating callose deposition [19]. FaERF2 activates *FaBG-1* and *FaBG-2* genes to enhance strawberry resistance to *Botrytis cinerea* [20]. Co-overexpression of chitinase and β-1,3-glucanase enhances wheat resistance to Fusarium [21].

Additionally, they exhibit important roles in regulating plant development and abiotic stress. For instance, *BGs* may play a role in banana fruit softening and be induced by hormones and stress [22]. Arabidopsis *PdBG1* and *PdBG2* are involved in regulating the number and distribution of lateral roots [23], while the *Drosera rotundifolia BG* gene is expressed in vegetative organs and function in the development of transgenic tobacco [24]. The destruction of *AtBG14* leads to increased deposition of callose in developing seeds and reduces seed longevity and dormancy [25]. *GhGLU18* promotes fiber cell elongation and secondary cell wall deposition in cotton [26]. *BGs* reduce solute influx into membrane vesicles during freezing, thereby reducing osmotic stress and vesicle rupture during thawing [27]. Cold and gibberellin can excessively induce BG to reopen signal channels and break the dormancy of poplar and *Paeonia suffruticosa* [28, 29]. Meanwhile, sugarcane *ScGluD2* is involved in plant defense against smut pathogen attack as well as responses to salt and heavy metal stress [30]. In addition to *BG* genes, promoter activity is also activated by stress or hormones. For example, the promoter of *Brassica juncea BjPR2* is induced by fungal infection, plant hormones and wounding [31], while the promoter of the sesame *BG* gene is induced by ABA and drought stress [32].

Grapes, as one of the world's widely cultivated economic fruit crops, are used for various purposes, including as a fresh and processed food. Cultivated grapevines usually exhibit low resistance to biotic and abiotic stress. *BG* genes have been shown to be extensively involved in plant responses to stress. Recently, *VviBG* genes in grapevines have been reported as cryoprotectants [33] and to play a role in resistance against different pathogens [34, 35]; however, a study of the identification and expression of *VviBG* gene family members in grapevines has not yet been reported. In this study, the *VviBG* family members were first identified, before undergoing chromosome localization, synteny analysis and phylogenetic analysis. Additionally, tissue specificity and expression levels of *VviBGs* under different stresses were analyzed using transcriptome data. Finally, the expression patterns of *VviBGs* under abiotic stress were investigated via RT-qPCR analysis. The identification and expression analysis of the *VviBG* family in our study laid a theoretical foundation for understanding their functions in grape resistance to different stresses.

## Methods

### Plant materials and treatments

The self-rooted cuttings of 'Thompson Seedless' were grown in a greenhouse (Henan Institute of Science and Technology) at 25–30℃ and 60–75% relative humidity. Two-month-old grape seedlings were selected for abiotic stress treatment. Grape seedlings were placed in an incubator at 4°C for cold treatment, irrigated with 10% PEG6000 for drought treatment, and irrigated with 150

mM NaCl for salt treatment. Grape seedlings grown in a controlled-environment chamber at 22℃ were used as controls. Samples were collected 0 h, 3 h, 6 h, 24 h and 48 h after treatment, with three biological replicates for each treatment. All leaf samples were immediately stored at -80°C for RNA extraction.

#### Identification of *VviBG* genes in grapevine

The amino acid sequence of the *AtBG* gene *AT4G14080* was obtained from the NCBI database (https://www.ncbi.nlm.nih.gov/), it contains two conserved domains GH17 and CBM43 of the *BG* gene family and used as query to search for homologous proteins in the grape genome (https://plants.ensembl.org/index.html) using the BLAST program. Candidate proteins were further subjected to multiple sequence alignment to remove duplicates and incomplete protein sequences. Finally, the identification of conserved domains was performed using NCBI CDD tools (https://www.ncbi.nlm.nih.gov/cdd) and the InterPro database (https://www.ebi.ac.uk/interpro/) to identify the *VviBG* gene family members in grapevine, which were named based on their chromosomal positions. The Protein Parameter Calc (ProtParam-based) function of TBtools [36] was used to analyze various parameters of the *VviBG* proteins. Glycosyl phosphatidyl isohydrin (GPI) anchor prediction was performed using PredGPI (https://busca.biocomp.unibo.it/predgp).

#### Chromosome localization and synteny analysis

Chromosome localization of *VviBGs* was visualized using Gene Location Visualize in TBtools. The homology and synteny of *VviBGs* were analyzed with default parameters (CPU for BlastP: 2, E-value:1e-10, Num of BlastHits: 5) using One Step MCScanX in TBtools and visualized with Advanced Circos in TBtools.

#### Bioinformatics analysis of *VviBGs*

The genomic, CDS and protein sequences of *VviBGs* were obtained from the grape genome database (https://plants.ensembl.org/index.html). Multiple sequence alignment of *VviBG* proteins was performed using ClustalX2.1. The phylogenetic tree was constructed with MEGA 7.0 using the neighbor-joining method and 1000 bootstrap replicates. The exon/intron analysis of *VviBGs* was conducted using the GSDS 2.0 (http://gsds.gao-lab.org/index.php). The motif analysis of *VviBGs* was performed in MEME (http://meme-suite.org/), with parameters set as follows: default for advanced options and a maximum of 12 motifs. The conserved domain identification of VviBGs was carried out using the CD-search of NCBI (https://www.ncbi.nlm.nih.gov/cdd).

#### Analysis of *cis*-elements of *VviBG* promoters

The upstream 2000 bp promoter sequences of *VviBGs* were obtained using TBtools, and PlantCARE (http://bioinformatics.psb.ugent.be/webtools/plantcare/html/) was used to predict the *cis*-elements of the *VviBG* promoters. Visualize and plotting of the types and numbers of *cis*-elements were then performed using Basic Biosequence View and Heatmap in TBtools, respectively.

#### Transcriptomic data analysis of *VviBGs*

Publicly available transcriptomic data (GSE36128) of 54 grape ('Corvina') samples comprising different tissues and developmental stages were utilized to analyze the tissue-specific expression patterns of *VviBGs*. Detailed information about grape different tissues and developmental stages can be found in the previous study [37]. Publicly available transcriptomic data (GSE37743) were used to analyze the expression patterns of *VviBGs* after 0 h, 24 h and 48 h of wounds, UV and pathogenic bacteria treatment in 'Pinot Noir' grape leaves. The information about the stress condition can be found in previous study [38]. Furthermore, our transcriptomic data (GSE276430) were analyzed to investigate the expression patterns of *VviBGs* at 0 h and 48 h after treatment with cold (4°C), drought (PEG6000) and salt (NaCl). Finally, the heatmaps of gene expression were generated using TBtools.

#### RT-qPCR analysis

Total RNA extraction of grape leaves and cDNA synthesis were performed using the EZNA Plant RNA Kit and M5 Super plus qPCR RT kit with gDNA remover (Agilent, China) respectively. The cDNA was diluted 5-fold at a concentration between 150 and 200 ng/uL and used for RT-qPCR reaction. RT-qPCR reactions were conducted using the SYBR qPCR Mixture (GenStar, China) and CFX Connect Real-Time PCR Detection System (Bio-Rad, USA). Each reaction was performed with three biological replicates. *VviGAPDH* (GU585870) and *VviACTIN* (AY680701) were attempted as reference genes, and finally *VviACTIN* was used as the reference gene. Relative expression levels were calculated using the $2^{-\Delta\Delta CT}$ method [39]. The primers used for RT-qPCR are listed in Table S1.

## Results

#### Identification and characterization of the *VviBG* gene family

Using the Arabidopsis AT4G14080 gene for BLAST, 73 homologous proteins were obtained in the grape genome, with 53 remaining after removing duplicates and short fragments. Finally, 42 members of the *VviBGs* in grapevine were identified through conserved domain analysis and named *VviBG1*–*VviBG42* based on their chromosomal positions (Table S2). In Table S2, it was

evident that the CDS length of *VviBGs* ranged from 837 (*VviBG20*) to 1584 bp (*VviBG33*), while the length of amino acids ranged from 290 to 527 aa. The molecular weights ranged from 32.24 to 57.67 kDa, and the isoelectric points ranged from 4.70 (*VviBG4*) to 9.39 (*VviBG19*). Among them, 12 *VviBGs* were unstable proteins with an instability index greater than 40. It was predicted that 14 *VviBGs* contained GPI anchor attachment.

### Chromosomal localization and synteny analysis of *VviBGs*

Tandem duplication and whole genome-duplication have been found to be important for the expansion of gene families [40]. In order to further verify the duplication events of the *VviBGs* during evolution, our study investigated the chromosomal localization and synteny relationships of the *VviBGs*. As shown in Fig. 1, *VviBGs* were unevenly distributed on 19 chromosomes, among which chromosomes 6, 8 and 11 contained more genes (6, 7 and 5, respectively). Additionally, four tandem repeat gene clusters were found within the *VviBGs*, with cluster sizes ranging from 2 to 3 genes. *VviBG11* and *VviBG12* formed a tandem repeat gene cluster on chromosome 6, while *VviBG15* and *VviBG16* as well as *VviBG17*, *VviBG18* and *VviBG19* formed tandem repeat gene clusters on chromosome 8. *VviBG41* and *VviBG42* were tandem repeat genes located on chromosome Un (Fig. 1, Table S3).

Synteny analysis revealed two whole-genome duplication regions in the grape genome: *VviBG5*/*VviBG39* and *VviBG32*/*VviBG40* (Fig. 2a and Table S4). To further infer the evolutionary relationships between *BG* family members, we constructed synteny analysis of *BG* gene families in grape and Arabidopsis (Fig. 2b and Table S4). A total of 20 *VviBG* genes in grape showed synteny with Arabidopsis, and some *VviBGs* showed a synteny relationship with two *AtBGs*, such as *VviBG5*, *VviBG21*, *VviBG26*, *VviBG29* and *VviBG40* (Table S4).

### Multiple sequence alignment and phylogenetic analysis of *VviBGs*

Multiple sequence alignment reveals conserved and functional associations among gene family members. Therefore, in our study, the multiple sequence alignment analysis of *VviBGs* was conducted (Figure S1). The results showed that all VviBG proteins contained an N-terminal signal peptide (except VviBG20) and a GH-17 domain, but the C-terminal sequences were not conserved. In Arabidopsis, based on the presence or absence of C-terminal structural features, AtBGs were divided into five types [4], while VviBGs in grape were divided into four types, lacking type III (Figure S2). There were 12 members in type I, containing the CBM43 domain and C-terminal hydrophobic sequence; 9 members in type II, containing the CBM43 domain; 6 members in type IV, containing C-terminal hydrophobic sequence; and 15 members in type V, lacking the C-terminal structural features.

To study the evolutionary relationship between *VviBGs* and *AtBGs*, phylogenetic analysis was performed (Fig. 3). The results showed that 42 *VviBGs* and *50 AtBGs* were classified into three clades (α, ß and γ), consistent with previous studies in Arabidopsis [4]. Among them, the α clade contained the largest number of *VviBGs*, with 20 members; followed by the γ clade, with 15 members; and finally, the ß clade, which contained 7 *VviBGs*. To better understand the evolutionary relationship of *VviBGs* in grape, phylogenetic analysis of *VviBGs* was conducted (Fig. 4a). The α, ß and γ clades were divided into 6 subgroups (A–F) according to the cotton [6].

### Analysis of motif/domain and gene structure of *VviBGs*

The motif analysis showed that the *VviBGs* exhibited strong conservation in the distribution pattern and quantity of motifs. *VviBGs* of the A, D and F subgroups

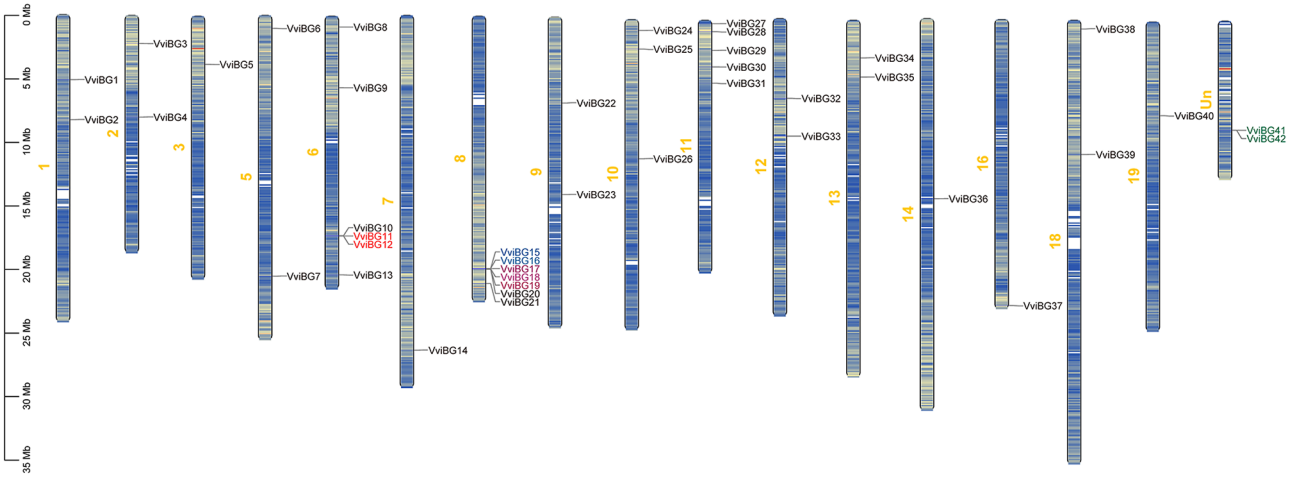


**Fig. 1** Chromosomal localization analysis of *VviBGs* in grapevine. *VviBGs* are sequentially numbered according to their positions on chromosomes: *VviBG1*–*VviBG42*. Tandem repeat gene clusters of *VviBGs* are marked with different colors. Chromosomal localization of *VviBGs* was visualized using TBtools

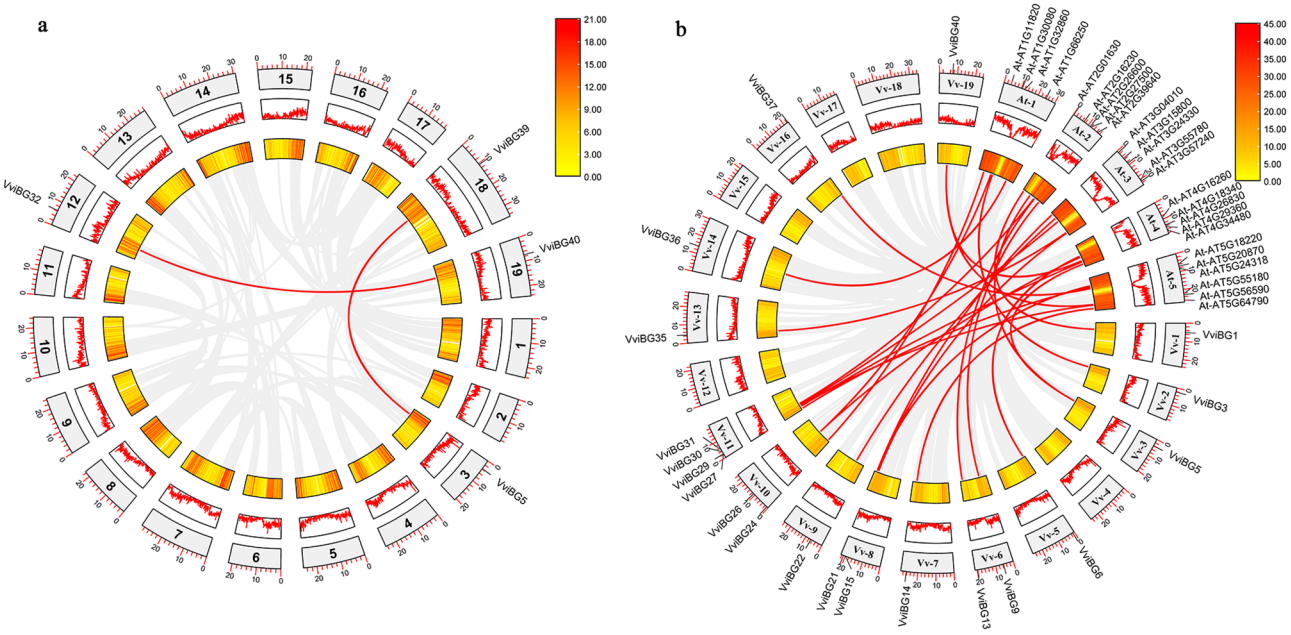


**Fig. 2** Synteny analysis of *VviBGs* within the grapevine and between grapevine and Arabidopsis. (**a**) Synteny analysis of *VviBGs* in grapevine. Gene pairs are connected by a red line. (**b**) Synteny analysis of *VviBGs* between grapevine and Arabidopsis. The red lines highlight the syntenic *VviBG* gene pairs. The chart was plotted with TBtools

contained 10 motifs, while *VviBGs* of the B, C and E subgroups contained 12 motifs (Fig. 4b). The conserved domain analysis indicated that 15 *VviBGs* of type V and 6 *VviBGs* of type IV containing the GH-17 domain were classified into subgroups A and D/F, respectively. 12 *VviBGs* of type I containing both GH-17 and CBM43 domains were classified into subgroups B (7 *VviBGs*) and C (5 *VviBGs*), while 9 *VviBGs* of group 2 containing GH-17 and CBM43 domains were classified into subgroups C (3 *VviBGs*) and E (6 *VviBGs*) (Fig. 4c). Gene structure analysis revealed that *VviBGs* of subgroups A and B both contained one intron, while *VviBG* genes of subgroups C, D and E contained varying numbers of introns ranging from 1 to 5. The F subgroup only contained *VviBG35*, which had no introns.

### Analysis of *cis*-acting elements in the promoters of *VviBGs*

In order to further analyze the functions of *VviBGs* in plant growth, development and stress response, the *cis*-acting elements of the *VviBG* promoters were analyzed (Fig. 5). In addition to the core promoter elements, a total of 33 types of elements were identified, categorized into four functional classes: light-responsive elements, stress-responsive elements (wounds, low temperature, stress, anaerobic and oxidative), hormone-responsive elements (gibberellin, auxin, abscisic acid, methyl jasmonate, salicylic acid and ethylene) and transcription factor binding elements (DREB, WRKY, MYB and MYC).

Then further analysis was conducted on the number of *cis*-acting elements contained in the promoter of *VviBGs* (Fig. 5c, Table S5). The results showed that the light-responsive element predominantly consisted of Box 4, with *VviBG2*, *VviBG9*, *VviBG20* and *VviBG42* containing up to eight. The main responsive elements included stress-responsive elements (STRE) and antioxidant-responsive elements (ARE), with each *VviBG* promoter in the ß clade containing 3–7 STRE elements, and each *VviBG* promoter in subgroup C of the α clade containing 1–6 ARE elements. The hormone-responsive elements mainly included ERE and ABRE, with almost all *VviBG* promoters containing ERE and ABRE, and *VviBG2* and *VviBG28* having the most ERE elements, with up to seven. The transcription factor binding elements mainly included MYC, present in almost all *VviBG* promoters, with *VviBG16*, *VviBG17*, *VviBG29*, *VviBG35* and *VviBG39* having the most (up to seven).

### RNA-seq analysis of tissue-specific expression patterns of *VviBGs*

To investigate the role of *VviBGs* in different tissues and developmental stages of grapevine, we analyzed the tissue-specific expression patterns of *VviBGs* in 54 grape ('Corvina') samples comprising different tissues and developmental stages using transcriptome data (GSE36128) (Fig. 6, Table S6). The results indicated that with the maturation of various tissues of grape, the expression of 5 *VviBGs* (*VviBG6*, *VviBG10*, *VviBG11*, *VviBG4* and *VviBG40*) and 15 *VviBGs* (*VviBG41*, *VviBG19*, *VviBG16*, *VviBG17*, *VviBG33*, *VviBG1*, *VviBG36*, *VviBG29*, *VviBG32*, *VviBG3*, *VviBG13*,

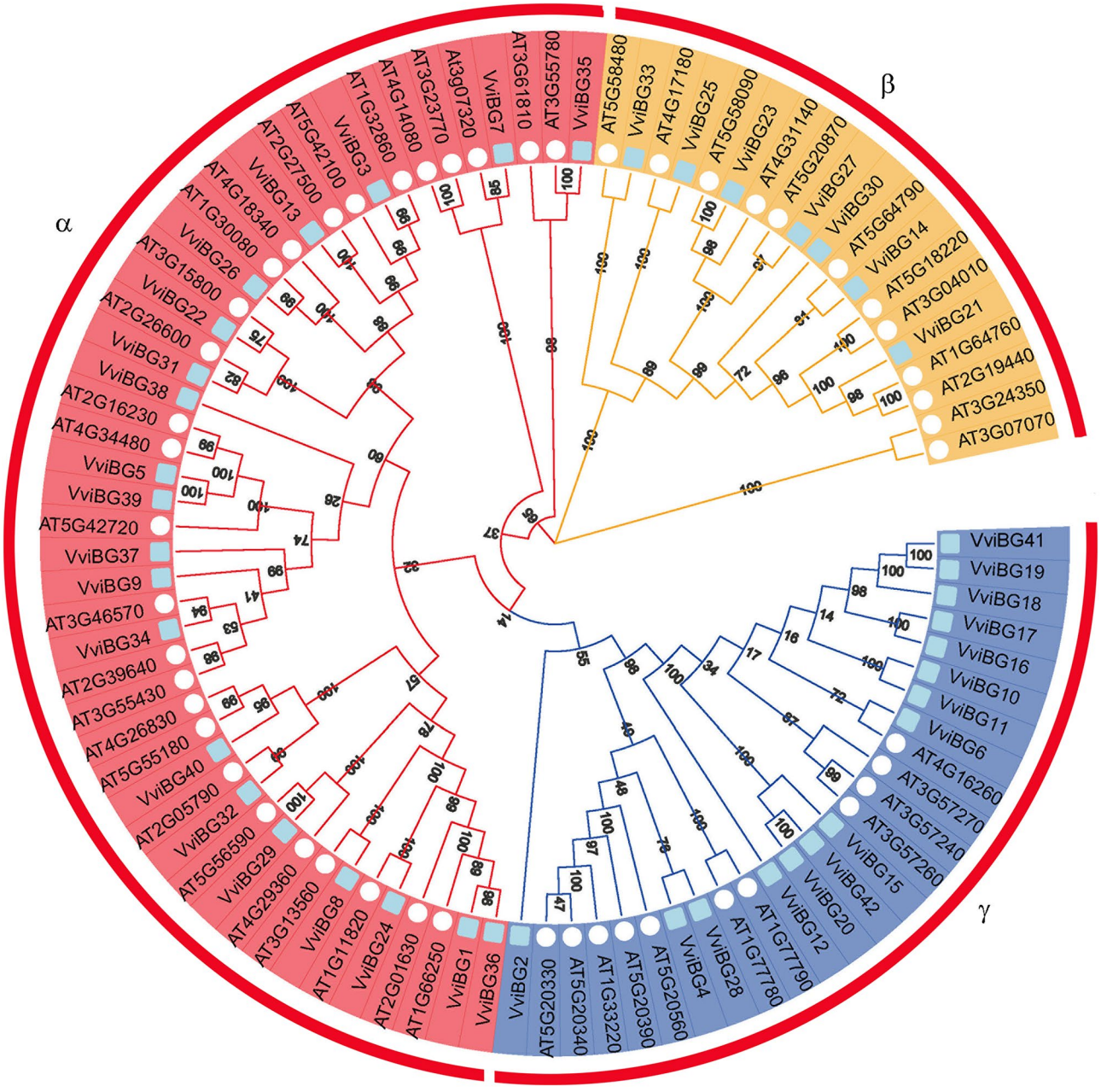


**Fig. 3** Phylogenetic analysis of grapevine and Arabidopsis *BG* genes. The phylogenetic tree was constructed using the neighbor-joining method in MEGA7.0, with a bootstrap value of 1000, and was visualized using Evolview

*VviBG31*, *VviBG38*, *VviBG5* and *VviBG39*) showed an increasing and decreasing trend, respectively. Genes such as *VviBG40*, *VviBG21*, *VviBG34*, *VviBG5*, *VviBG3*, *VviBG32*, *VviBG23* and *VviBG39* were highly expressed in almost all tissues, while *VviBG9* and *VviBG12* showed very low expression levels in almost all tissues. Some *VviBGs* exhibited similar expression patterns in different tissues, such as *VviBG7* and *VviBG8*, *VviBG2* and *VviBG14*, *VviBG28* and *VviBG35*, *VviBG10* and *VviBG11*, *VviBG19* and *VviBG41*, *VviBG16* and *VviBG17*, *VviBG20* and *VviBG42*. Some genes also exhibited tissue-specific expression, such as *VviBG2* and *VviBG14*, which had relatively high expression levels in flower organs (stamen, pollen and flower), *VviBG12*, which was mainly highly expressed in tendril WD, and *VviBG10*, which was mostly expressed in roots.

### RNA-seq analysis of expression patterns of *VviBGs* under wounds, UV and downy mildew stress

To determine the expression of *VviBGs* under different stresses, the RNA-seq data (GSE37743) of 'Pinot Noir' leaves under wounds, UV and downy mildew stress were

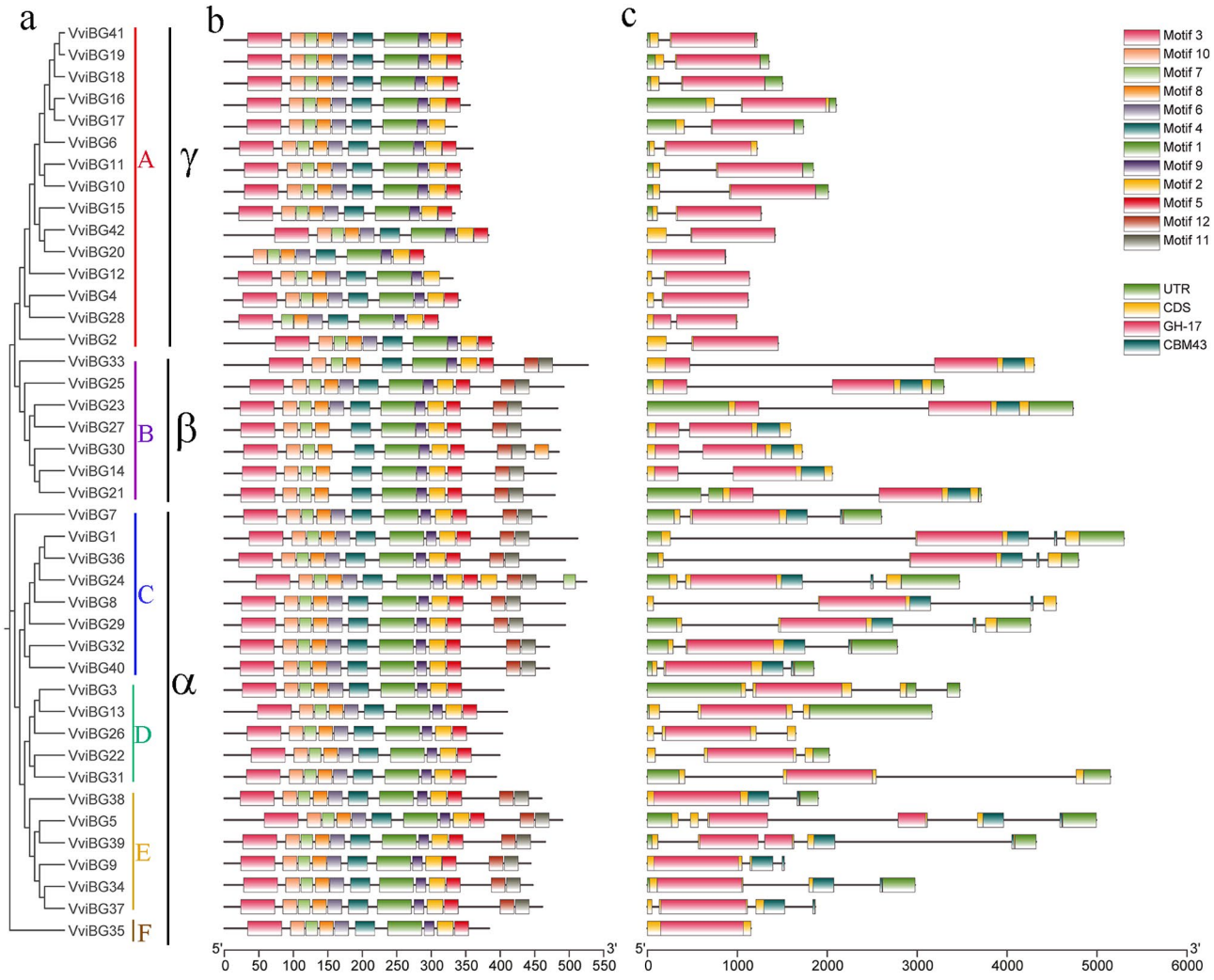


**Fig. 4** Phylogenetic, motif, conserved domain and gene structure analysis of the *VviBGs* in grapevine. (**a**) Phylogenetic analysis of *VviBGs*. (**b**) Motif analysis of *VviBGs*. (**c**). Conserved domain and gene structure analysis of *VviBGs*. Visualization was performed using TBtools

analyzed (Fig. 7, Table S7). The results revealed that 35 *VviBGs* were significantly induced or inhibited under at least one of the stresses. Ten *VviBGs* (*VviBG4*, *VviBG6*, *VviBG10*, *VviBG11*, *VviBG16*, *VviBG17*, *VviBG18*, *VviBG19*, *VviBG40* and *VviBG41*) and two *VviBGs* (*VviBG15* and *VviBG36*) were significantly induced and inhibited under all three stresses at 24 h and 48 h. Some *VviBG* genes were induced by two stresses, namely *VviBG1*, *VviBG3*, *VviBG23*, *VviBG33* and *VviBG38* were significantly induced by wounds and downy mildew; *VviBG22* and *VviBG26* were significantly induced by wounds and UV; *VviBG2*, *VviBG29* and *VviBG37* were significantly induced by UV and downy mildew. On the other hand, some genes were inhibited by one or two stress, such as *VviBG20* and *VviBG42* were significantly inhibited by wounds and downy mildew. *VviBG31* was significantly inhibited by wounds, *VviBG3* and *VviBG27* were significantly inhibited by downy mildew, and *VviBG5*, *VviBG8*, *VviBG13*, *VviBG30*, *VviBG32*, *VviBG34* and *VviBG39* were significantly inhibited by UV.

### RNA-seq analysis of expression of *VviBGs* under abiotic stress

Previously, we performed RNA-seq analysis on 'Thompson Seedless' leaves treated with three abiotic stresses (cold, PEG6000 and NaCl) (GSE276430). Then, the expression of *VviBGs* under abiotic stresses was analyzed utilizing the RNA-seq data (Fig. 8, Table S7). It was found that after 48 h of cold treatment, the expression levels of 10 *VviBGs* (*VviBG4*, *VviBG6*, *VviBG10*, *VviBG11*, *VviBG19*, *VviBG21*, *VviBG22*, *VviBG26*, *VviBG34* and *VviBG40*) and 3 *VviBGs* (*VviBG32*, *VviBG33* and *VviBG37*) increased and decreased, respectively. Among them, *VviBG4* exhibited the highest induced fold change, although it was almost not expressed in the control. We also found that the expression levels

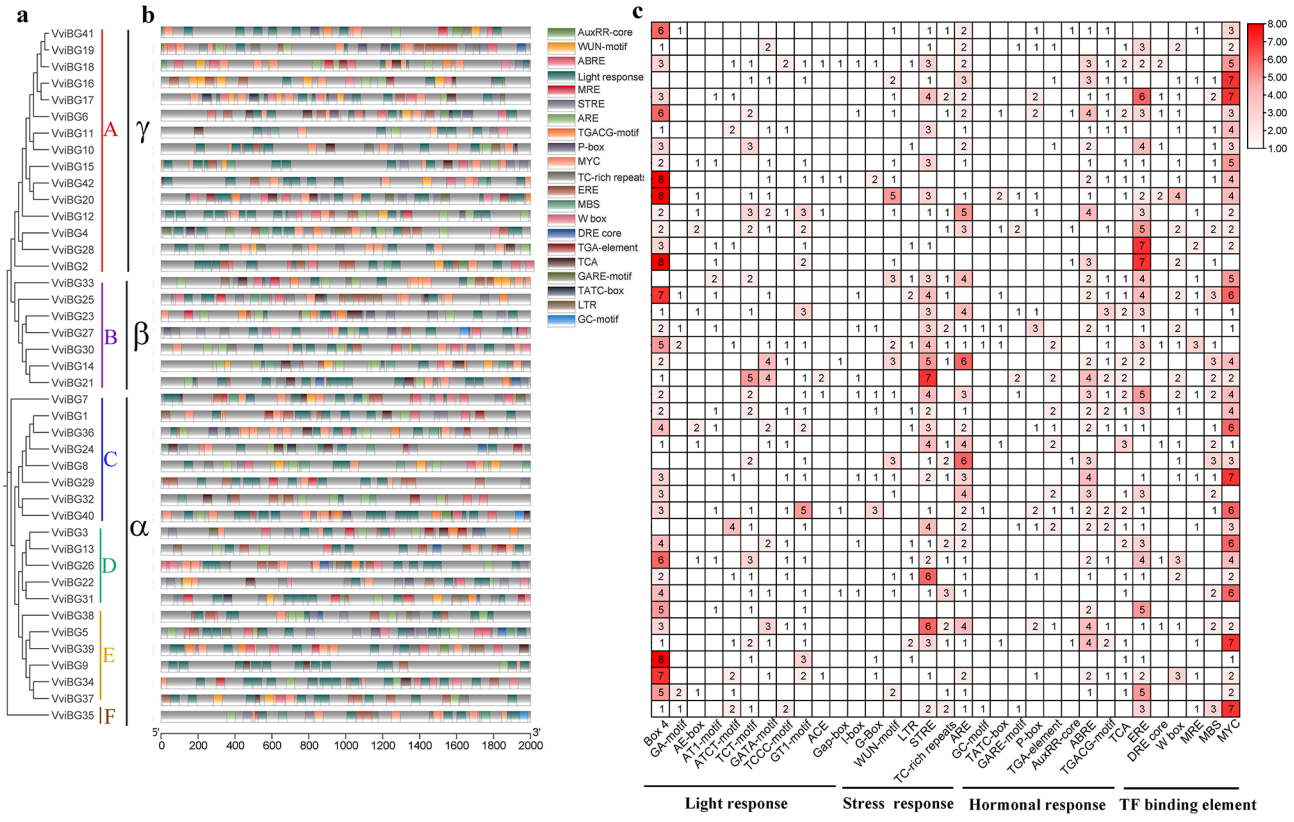


**Fig. 5** Analysis of the types and numbers of *cis*-acting elements in the promoters of *VviBGs*. (**a**) Phylogenetic analysis of *VviBGs*. (**b**) Schematic diagram of *cis*-acting elements in the *VviBG* promoters. (**c**) Heatmap analysis of the numbers of *cis*-acting elements in the *VviBG* promoters. Visualization was performed using TBtools

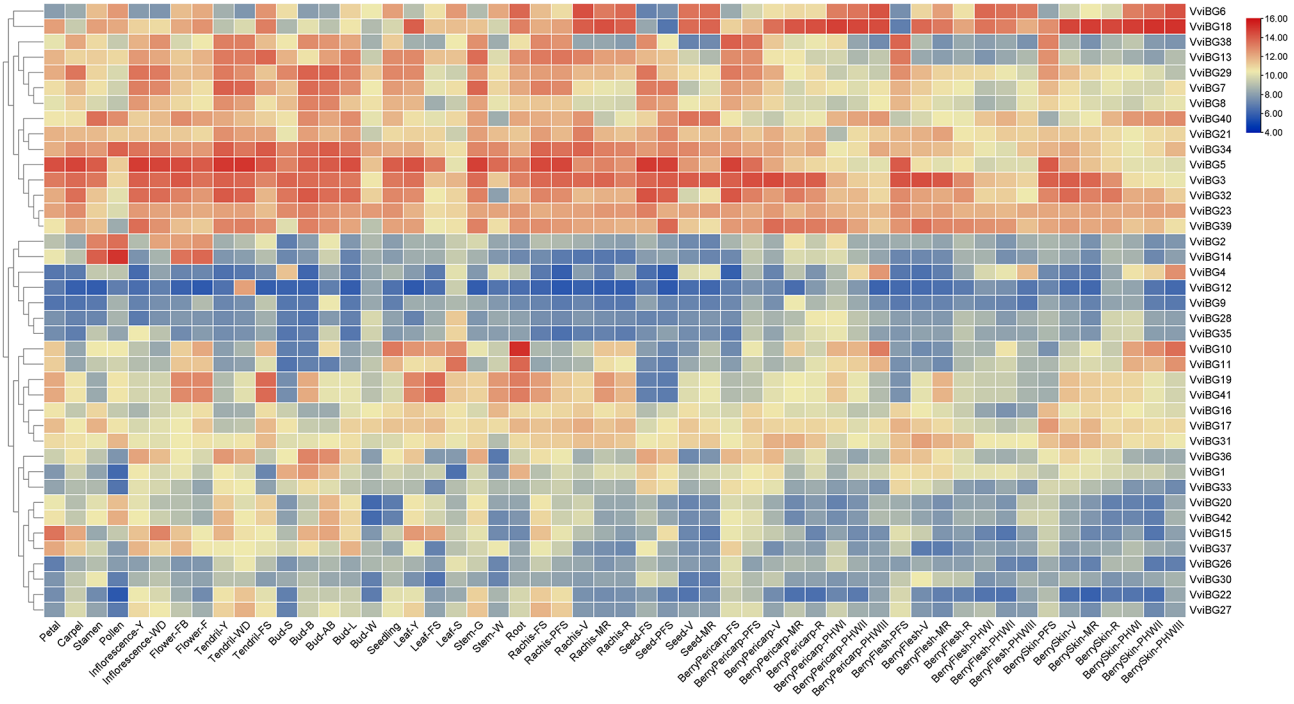


**Fig. 6** Expression patterns of *VviBGs* in 54 different grapevine tissue samples. The transcriptome data were obtained from the grapevine expression database GSE37743. Log2 (RNA-normalized value + 1) was used to indicate the gene expression values. Heatmap visualization was performed using TBtools

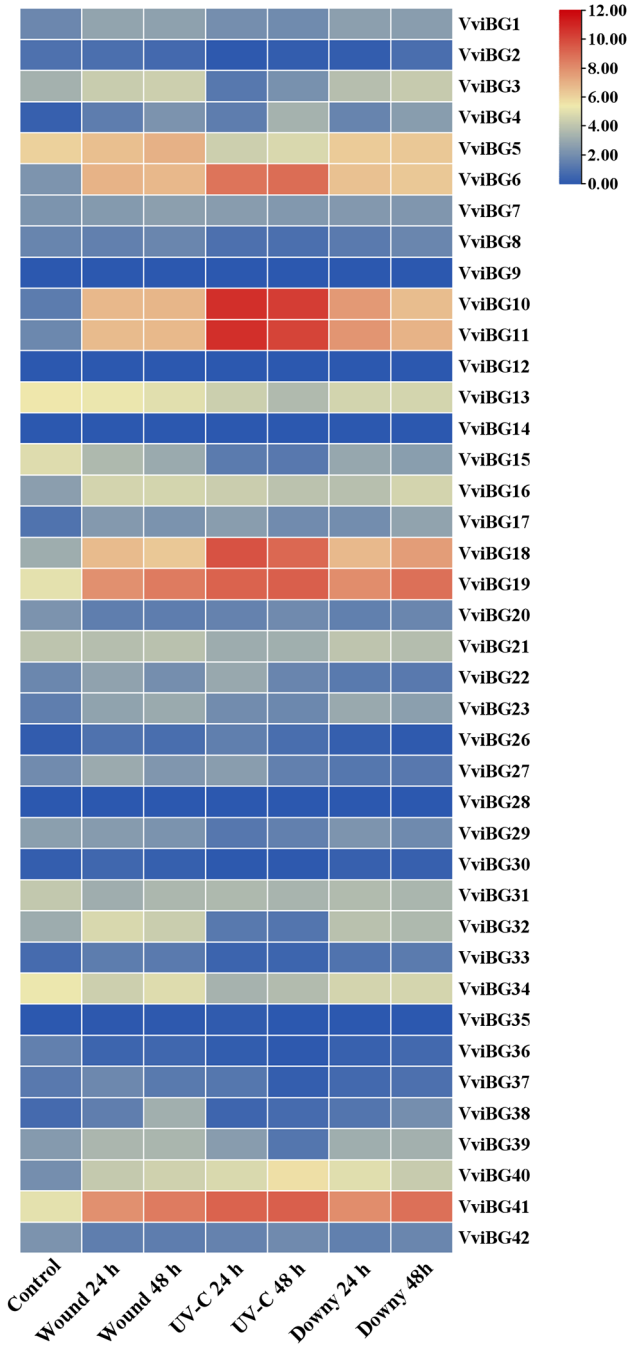


**Fig. 7** Analysis of expression patterns of *VviBGs* under wounds, UV and downy mildew stress. The transcriptome data were obtained from the grapevine expression database GSE37743. Log2 (RNA-normalized value + 1) was used to indicate the gene expression values. Heatmap visualization was performed using TBtools

of 10 *VviBGs* (*VviBG6*, *VviBG10*, *VviBG11*, *VviBG16*, *VviBG17*, *VviBG18*, *VviBG19*, *VviBG26*, *VviBG34* and *VviBG41*) and 7 *VviBGs* (*VviBG8*, *VviBG13*, *VviBG25*, *VviBG29*, *VviBG32*, *VviBG33* and *VviBG36*) increased and decreased respectively after PEG6000 treatment for 48 h, and *VviBG11* was induced to express at the highest fold. Finally, it was shown that after 48 h of NaCl treatment, the expression levels of 6 *VviBGs* (*VviBG6*, *VviBG10*, *VviBG11*, *VviBG17*, *VviBG19* and *VviBG41*) and 2 *VviBGs* (*VviBG13* and *VviBG32*) increased and decreased, respectively, with *VviBG10* exhibiting the highest induced fold change. Meanwhile, we observed that *VviBG6*, *VviBG10*, *VviBG11* and *VviBG19* were induced by all three abiotic stresses, *VviBG26* and *VviBG34* were induced by cold and PEG6000, and *VviBG17* and *VviBG41* were induced by PEG6000 and NaCl.

### RT-qPCR analysis of expression patterns of *VviBGs* under abiotic stress

Based on the transcriptome data analysis of abiotic stress, eight genes (*VviBG6*, *VviBG10*, *VviBG11*, *VviBG16*, *VviBG17*, *VviBG18*, *VviBG19* and *VviBG41*) were selected from subgroup A of the γ clade for RT-qPCR analysis (Fig. 9). The results showed that the eight genes were induced by all three abiotic stresses, except for *VviBG41* under 4°C. Most *VviBGs* were not significantly induced at 3 h of abiotic stress and were even suppressed; however, with prolonged treatment time, *VviBG6*, *VviBG10*, *VviBG11* and *VviBG19* showed the highest induction after 48 h of the three stresses. Furthermore, most genes among the eight *VviBGs* showed a higher induction by PEG6000 and NaCl compared to 4°C, such as *VviBG6*, *VviBG10*, *VviBG11*, *VviBG16*, *VviBG19* and *VviBG41*.

## Discussion

BGs are localized in various organs at different developmental and reproductive stages of plants, playing crucial roles in cell division, intercellular transport, flower formation, seed maturation and defense against biotic and abiotic stresses [41]. Studies have shown that overexpression of flax *BGs* leads to accumulation of pectin and phenolic substances, resulting in higher antioxidant capacity [42]. We speculated that *VviBGs* may also enhance grape antioxidant capacity in this way and thereby increase stress resistance. Our study identified 42 *VviBGs* in grape, twelve *VviBGs* of type I and six *VviBGs* of type IV contain C-terminal hydrophobic sequences encoding transient transmembrane domains, among which 14 genes contain GPI anchor attachments (Table S2), indicating that they may be localized to vacuoles [43] or the plasma membrane/cell wall [44, 45].

Four pairs of *VviBG* tandem repeats were detected in the grape genome (Fig. 1), suggesting that they were involved in the expansion of the *VviBG* gene family. Synteny analysis (Fig. 2a) revealed that proteins corresponding to *VviBG5* and *VviBG39* or *VviBG32* and *VviBG40* may have similar functions. The existence of one-to-many synteny relationships between *VviBGs* and

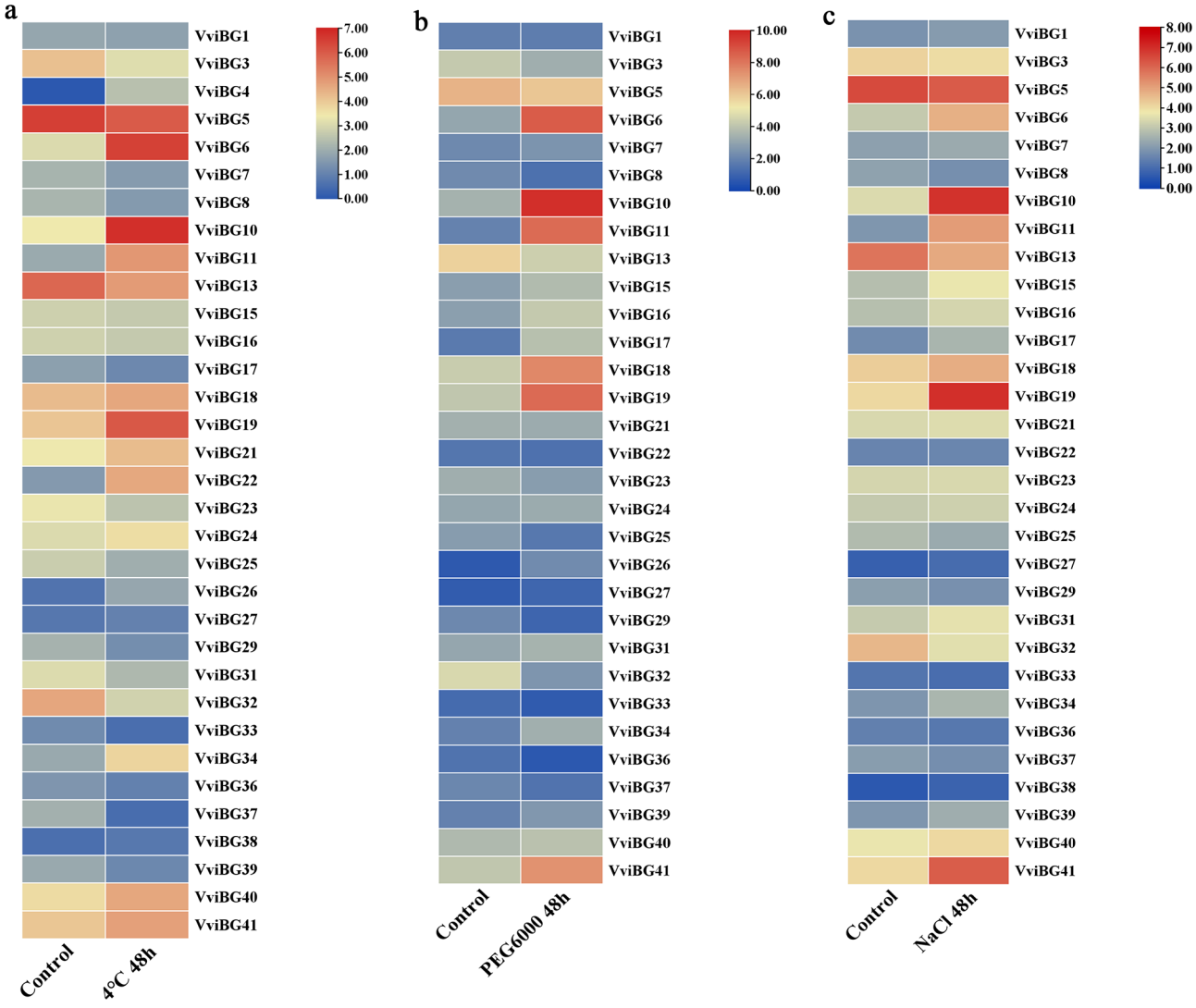


**Fig. 8** Expression patterns of *VviBGs* under cold (**a**), PEG6000 (**b**) and NaCl (**c**) treatments. Log2 (RNA-normalized value + 1) was used to indicate the gene expression values. Heat map visualization was performed using TBtools

*AtBGs* (Fig. 2b) suggested that *VviBGs* may have multiple orthologous genes in Arabidopsis, while also indicating a reduction in the number of *VviBGs* during evolution. *VviBGs* were divided into four types, lacking type III (Figure S2), indicating that *VviBGs* may have lost genes with two CBM43 domains during grapevine evolution.

Different types of *cis*-acting elements on the promoter reveal the potential functions and regulatory differences of genes. We found that the *VviBG* promoters contained many elements related to stress and hormone responses (Fig. 5). STRE responds to various stress conditions including heat, high osmotic pressure and ethanol [46]. ß clade *VviBG* promoters contained high amounts of STRE, suggesting that these genes may confer grape stress resistance by responding to external stresses. On the other hand, ARE belongs to antioxidant response elements [47], the α clade *VviBG* promoters contained many ARE elements, indicating that they may confer grape stress resistance through oxidative stress pathways. ERE and ABRE denote ethylene and abscisic acid response elements, respectively, and almost all *VviBG* promoters were found to contain these two hormones, suggesting that they play a major role in regulating *VviBGs* in grape growth, development and stress response. The *VviBG* promoters also contained many transcription factor binding elements, in the future, the upstream transcription factors of *VviBGs* can be identified to explore the regulatory mechanism of *VviBGs*. The promoter activity of *BG* in other species is also induced by stress and hormones, such as the promoter of *BjPR2* being induced by fungi, hormones and wounds [31], or the *BG* gene promoter of sesame being induced by ABA and drought [32]. This indicates that the regulatory mechanism of *BG*

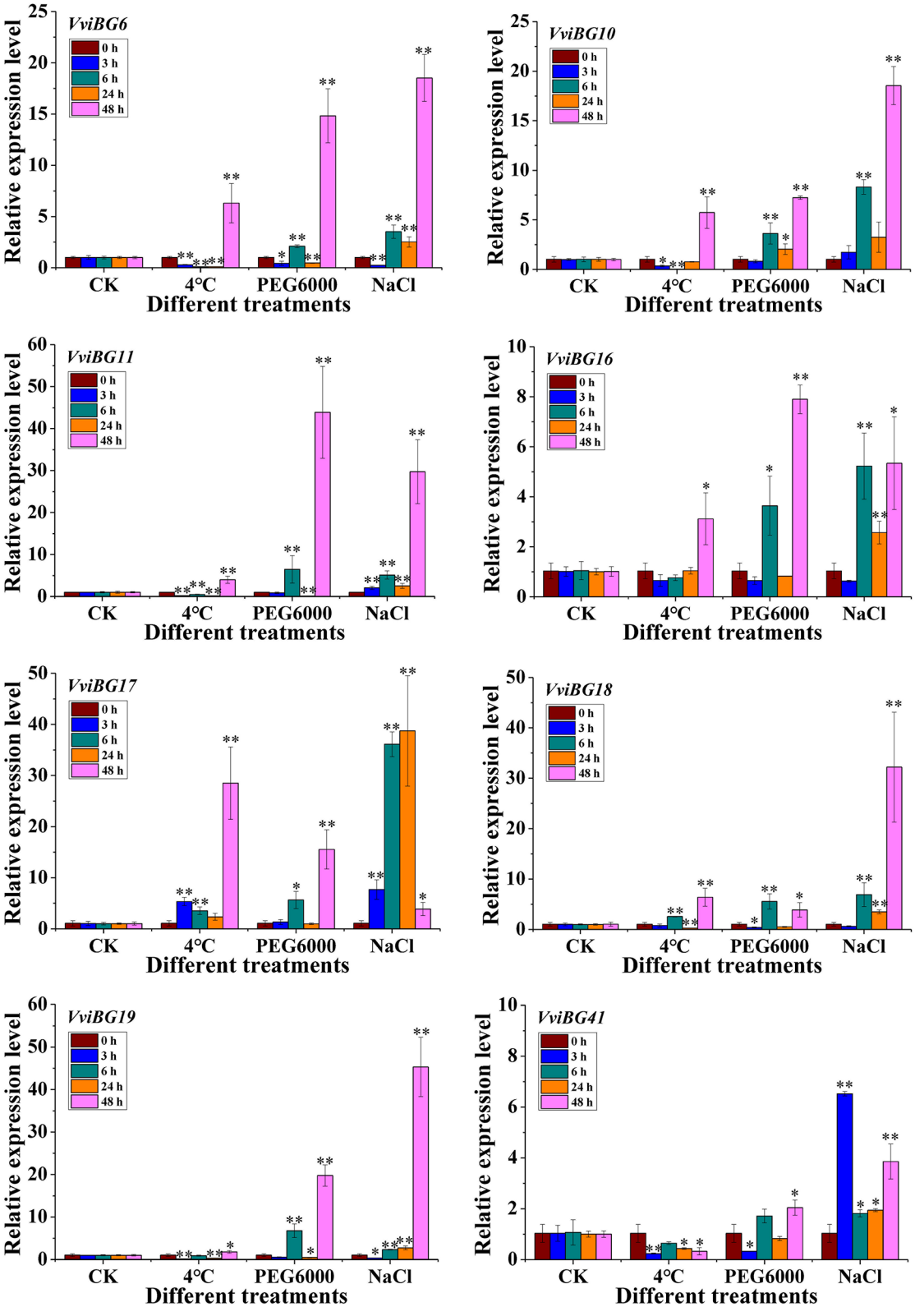


**Fig. 9** RT-qPCR analysis of *VviBGs* expression under 4°C, PEG6000 and salt treatments. Values represent the average of three biological replicates ± SD. Significance differences are indicated by asterisks (*$P < 0.05$ or **$P < 0.01$)

promoters in plant growth and stress response is relatively conservative.

In our study, 5 *VviBGs* and 15 *VviBGs* showed a trend of increasing and decreasing with the maturation of various tissues, respectively, indicating that they may play opposite roles at different stages of grape. Gene expression analysis suggests that *VviBG18* may play a key role in flower organ development, berry maturation and postharvest processes; *VviBG2* and *VviBG14* may mainly participate in flower and male organ development; *VviBG12* and *VviBG10* may play a role in the tendrils lignification and root development of grape, respectively. We also found that during the maturation process of various tissues, the induced *VviBGs* were mainly concentrated in the γ clade, while the inhibited *VviBGs* were mainly concentrated in the α clade, suggesting that *VviBGs* from the same clades may play similar roles in grape development. *VviBG7* and *VviBG8*, *VviBG2* and *VviBG14*, *VviBG28* and *VviBG35* showed distant phylogenetic relationships in the phylogenetic analysis, but exhibited similar expression profiles, which revealed that *VviBGs* with distant relationships may play similar roles in grape growth and development.

The transcriptome analysis (Fig. 7, Table S7) indicated that *VviBG6*, *VviBG10*, *VviBG11* and *VviBG18* may play a crucial role in grape response to wounds, UV and pathogens, especially *VviBG10*. The transcriptome analysis (Fig. 8, Table S8) also revealed that *VviBG6*, *VviBG10*, *VviBG11* and *VviBG19* may be involved in the grape response to abiotic stress (4℃, PEG6000 and salt), especially drought stress. *AtBG* gene At4g16260 is induced by pathogens and may play a role under drought and salt stress, as the drought and salt stress positive regulatory factor AtbHLH112 binds to the At4g16260 promoter [48]. This shows that the results of our study are consistent with Arabidopsis, as we found that *VviBG6* and At4g16260 are orthologous genes, and may have similar functions.

To date, there have been many studies on the disease resistance of *BGs*; however there are few studies on their function and mechanism under abiotic stress. RT-qPCR analysis (Fig. 9) showed that the expression of 8 *VviBGs* of subgroup A in the γ clade mainly increased in the later stages of 4℃, drought and salt treatments, especially at 48 h, indicating that the *VviBGs* may not take effect until some time after treatments. *VviBG6*, *VviBG11* and *VviBG19* were highly expressed under drought and salt stress, suggesting they may play a significant role under these two stresses. *VviBG18* was significantly upregulated under salt stress compared to the other two stresses, indicating that it may mainly play a role in the response to salt stress. *VviBG17* was induced to have the highest expression fold at 4℃, so it may be involved in the response to cold stress. According to the induced expression fold of *VviBG* genes, we also found that most genes may play a greater role in the response to drought and salt stress than cold stress.

## Conclusion

Our study identified 42 *VviBGs* in grapevine, all containing a GH-17 domain and C-terminal non conserved sequence features. We divided these into three clades α, ß and γ, and six subgroups. There were four tandem repeat gene clusters in the *VviBG* gene family, two pairs of synteny relationships in grapevine and twenty pairs of synteny relationships between grape and Arabidopsis. The *VviBG* promoters contained many *cis*-acting elements related to stress and hormone responses. *VviBGs* exhibited distinct spatial and temporal organization-specific expression patterns. Most *VviBGs* were induced by wounds, UV, pathogens, cold, salt, and drought, especially the 8 *VviBGs* in subgroup A. Most of the 8 *VviBGs* were induced by PEG6000 and NaCl with expression multiple times higher than those induced by cold. The comprehensive analyses of the *VviBG* gene family in grapevine will help to further elucidate the role of *VviBGs* in the grape responses to biotic and abiotic stress.

### Abbreviations

| | |
|---|---|
| ARE | Antioxidant-responsive elements |
| BG | β-1,3-glucanase |
| CalS | Callose synthase |
| GH-17 | Glycosyl hydrolase family 17 |
| GPI | Glycosyl phosphatidyl isohydrin |
| PD | Plasmodesmata |
| PR | Pathogenesis-related |
| STRE | Stress-responsive elements |

## Supplementary Information

The online version contains supplementary material available at https://doi.org/10.1186/s12870-024-05597-1.

Supplementary Material 1

Supplementary Material 2

Supplementary Material 3

Supplementary Material 4

Supplementary Material 5

Supplementary Material 6

Supplementary Material 7

Supplementary Material 8

Supplementary Material 9

Supplementary Material 10

Supplementary Material 11

### Acknowledgements

Not applicable.

**Author contributions**
LW and GL conceived and designed the experiments. LW, RL and ZQ performed the experiments. LW, KL, GL and PL analyzed the data and manuscript modification. RZ and GL contributed reagents/materials/analysis tools. LW contributed to the writing of the manuscript.

**Funding**
This work was supported by the Key Research and Development Program of Henan Province, China (241111113200), the R&D and Promotion Program (Science and Technology Research Project) of Henan Province, China (242102110319) and the Project 2 of the High Level Talent Introduction Program (103020224001/065).

**Data availability**
The data presented in the study are deposited in the NCBI repository, GEO accession: GSE276430.

## Declarations

**Ethics approval and consent to participate**
Not applicable.

**Consent for publication**
Not applicable.

**Competing interests**
The authors declare no competing interests.

Received: 27 June 2024 / Accepted: 16 September 2024
Published online: 01 October 2024

**References**

1. Chen X-Y, Kim J-Y. Callose synthesis in higher plants. Plant Signal Behav. 2009;4(6):489–92.
2. Linthorst HJ, Melchers SL, Mayer A, et al. Analysis of gene families encoding acidic and basic beta-1,3-glucanases of tobacco. Proc Natl Acad Sci U S A. 1990;87(22):8756–60.
3. Jin W, Horner HT, Palmer RG, et al. Analysis and mapping of gene families encoding beta-1,3-glucanases of soybean. Genetics. 1999;153(1):445–52.
4. Doxey AC, Yaish MWF, Moffatt BA, et al. Functional divergence in the Arabidopsis β-1,3-Glucanase gene family inferred by phylogenetic reconstruction of expression states. Mol Biol Evol. 2007;24(4):1045–55.
5. Wan L, Zha W, Cheng X, et al. A rice β-1,3-glucanase gene *Osg1* is required for callose degradation in pollen development. Planta. 2011;233(2):309–23.
6. Xu X, Feng Y, Fang S, et al. Genome-wide characterization of the β-1,3-glucanase gene family in Gossypium by comparative analysis. Sci Rep. 2016;6(1):29044.
7. Shinshi H, Wenzler H, Neuhaus JM, et al. Evidence for N- and C-terminal processing of a plant defense-related enzyme: primary structure of tobacco prepro-beta-1,3-glucanase. Proc Natl Acad Sci U S A. 1988;85(15):5541–5.
8. Payne G, Ward E, Gaffney T, et al. Evidence for a third structural class of beta-1,3-glucanase in tobacco. Plant Mol Biol. 1990;15(6):797–808.
9. Beffa RS, Neuhaus JM, Meins F Jr. Physiological compensation in antisense transformants: specific induction of an ersatz glucan endo-1,3-beta-glucosidase in plants infected with necrotizing viruses. Proc Natl Acad Sci U S A. 1993;90(19):8792–6.
10. Liu YF, Liu LJ, Yang S, et al. Molecular characterization and functional analysis of a pathogenesis-related β-1,3-glucanase gene in spruce. Eur J Plant Pathol. 2022;164(2):177–92.
11. Liu D, He X, Li W, et al. A β-1,3-glucanase gene expressed in fruit of *Pyrus pyrifolia* enhances resistance to several pathogenic fungi in transgenic tobacco. Eur J Plant Pathol. 2013;135(2):265–77.
12. Qiao LX, Ding X, Wang HC, et al. Characterization of the β-1,3-glucanase gene in peanut (*Arachis hypogaea* L.) by cloning and genetic transformation. Genet Mol Res. 2014;13(1):1893–904.
13. Gao L, Wang S, Zhang Y, et al. Identification and characterization of a β-1,3-glucanase gene, *TcLr19Glu*, involved in wheat resistance against *Puccinia Triticina*. J Plant Biochem Biot. 2016;25(3):319–26.
14. Zhang S, Zhang W, Zhai H, et al. Expression of a wheat β-1,3-glucanase in *Pichia pastoris* and its inhibitory effect on fungi commonly associated with wheat kernel. Protein Expres Purif. 2019;154:134–9.
15. Taif S, Zhao Q, Pu L, et al. A β-1,3-glucanase gene from *Panax notoginseng* confers resistance in tobacco to *Fusarium solani*. Ind Crop Prod. 2020;143:111947.
16. Wang Y, Liu M, Wang X, et al. A novel β-1,3-glucanase Gns6 from rice possesses antifungal activity against *Magnaporthe oryzae*. J Plant Physiol. 2021;265:153493.
17. Jha Y, Dehury B, Kumar SPJ, et al. Delineation of molecular interactions of plant growth promoting bacteria induced β-1,3-glucanases and guanosine triphosphate ligand for antifungal response in rice: a molecular dynamics approach. Mol Biol Rep. 2022;49(4):2579–89.
18. Felipe JEL, Lachica JAP, Dela Cueva FM, et al. Validation and molecular analysis of β-1,3-GLU2 SNP marker associated with resistance to *Colletotrichum gloeosporioides* in mango (*Mangifera indica* L). Physiol Mol Plant P. 2022;118:101804.
19. Pei Y, Xue Q, Zhang Z, et al. β-1,3-GLUCANASE10 regulates tomato development and disease resistance by modulating callose deposition. Plant Physiol. 2023;192(4):2785–802.
20. Peng Y, Liang M, Zhang X, et al. FaERF2 activates two β-1,3-glucanase genes to enhance strawberry resistance to *Botrytis Cinerea*. Plant Sci. 2024;347:112179.
21. Mohammadizadeh-Heydari N, Tohidfar M, Zanjani M. Co-overexpression of chitinase and β-1,3-glucanase significantly enhanced the resistance of Iranian wheat cultivars to Fusarium. BMC Biotechnol. 2024;24(1):35.
22. Choudhury SR, Roy S, Singh SK, et al. Molecular characterization and differential expression of β-1,3-glucanase during ripening in banana fruit in response to ethylene, auxin, ABA, wounding, cold and light-dark cycles. Plant Cell Rep. 2010;29(8):813–28.
23. Benitez-Alfonso Y, Faulkner C, Pendle A, et al. Symplastic intercellular connectivity regulates lateral root patterning. Dev Cell. 2013;26(2):136–47.
24. Michalko J, Renner T, Mészáros P, et al. Molecular characterization and evolution of carnivorous sundew (*Drosera rotundifolia* L.) class V β-1,3-glucanase. Planta. 2017;245(1):77–91.
25. Wang C, Lyu Y, Zhang Q, et al. Disruption of BG14 results in enhanced callose deposition in developing seeds and decreases seed longevity and seed dormancy in Arabidopsis. Plant J. 2023;113(5):1080–94.
26. Fang S, Shang X, He Q, et al. A cell wall-localized β-1,3-glucanase promotes fiber cell elongation and secondary cell wall deposition. Plant Physiol. 2023;194(1):106–23.
27. Hincha DK, Meins F Jr, Schmitt JM. β-1,3-Glucanase is cryoprotective in vitro and is accumulated in leaves during cold acclimation. Plant Physiol. 1997;114(3):1077–83.
28. Rinne PLH, Welling A, Vahala J, et al. Chilling of dormant buds hyperinduces FLOWERING LOCUS T and recruits GA-inducible 1,3-β-Glucanases to reopen signal conduits and release dormancy in populus. Plant Cell. 2011;23(1):130–46.
29. Gao X, Yuan Y, Liu Z, et al. Chilling and gibberellin acids hyperinduce β-1,3-glucanases to reopen transport corridor and break endodormancy in tree peony (*Paeonia suffruticosa*). Plant Physiol Biochem. 2021;167:771–84.
30. Su Y, Wang Z, Liu F, et al. Isolation and characterization of ScGluD2, a new sugarcane beta-1,3-Glucanase D family gene induced by *Sporisorium scitamineum*, ABA, $H_2O_2$, NaCl, and $CdCl_2$ stresses. Front. Plant Sci. 2016;7:1348.
31. Ali S, Chandrashekar N, Rawat S, et al. Isolation and molecular characterization of pathogenesis related *PR2* gene and its promoter from *Brassica juncea*. Biol Plant. 2017;61(4):763–73.
32. Parveen S, Mazumder M, Bhattacharya A, et al. Identification of anther-specific genes from sesame and functional assessment of the upstream region of a tapetum-specific β-1,3-glucanase gene. Plant Mol Biol Rep. 2018;36(2):149–61.
33. Romero I, Fernandez-Caballero C, Goñi O, et al. Functionality of a class I beta-1,3-glucanase from skin of table grapes berries. Plant Sci. 2008;174(6):641–8.
34. Mestre P, Arista G, Piron MC, et al. Identification of a *Vitis vinifera* endo-β-1,3-glucanase with antimicrobial activity against *Plasmopara Viticola*. Mol Plant Pathol. 2017;18(5):708–19.
35. Soon-Young A, Kim SA, Yun H. Differential expression of β -1,3-Glucanase transcripts induced by pathogens in the leaves of *Vitis Flexuosa*. Plant Breed Biotechnol. 2014;2(2):176–83.
36. Chen C, Wu Y, Li J, et al. TBtools-II: a one for all, all for one bioinformatics platform for biological big-data mining. Mol Plant. 2023;16(11):1733–42.

37. Fasoli M, Dal Santo S, Zenoni S, et al. The grapevine expression atlas reveals a deep transcriptome shift driving the entire plant into a maturation program. Plant Cell. 2012;24(9):3489–505.
38. Vannozzi A, Dry IB, Fasoli M, et al. Genome-wide analysis of the grapevine stilbene synthase multigenic family: genomic organization and expression profiles upon biotic and abiotic stresses. BMC Plant Biol. 2012;12(1):130.
39. Livak KJ, Schmittgen TD. Analysis of relative gene expression data using real-time quantitative PCR and the 2(T)(-Delta Delta C) method. Methods. 2001;25(4):402–8.
40. Kong H, Landherr LL, Frohlich MW, et al. Patterns of gene duplication in the plant *SKP1* gene family in angiosperms: evidence for multiple mechanisms of rapid gene birth. Plant J. 2007;50(5):873–85.
41. Balasubramanian V, Vashisht D, Cletus J, et al. Plant β-1,3-glucanases: their biological functions and transgenic expression against phytopathogenic fungi. Biotechnol Lett. 2012;34(11):1983–90.
42. Wojtasik W, Kulma A, Dyminska L, et al. Fibres from flax overproducing β-1,3-glucanase show increased accumulation of pectin and phenolics and thus higher antioxidant capacity. BMC Biotechnol. 2013;13:10.
43. Sticher L, Hinz U, Meyer AD, et al. Intracellular transport and processing of a tobacco vacuolar β-1,3-glucanase. Planta. 1992;188(4):559–65.
44. Henrissat B, Davies GJ. Glycoside hydrolases and glycosyltransferases. Families, modules, and implications for genomics. Plant Physiol. 2000;124(4):1515–9.
45. Borner GHH, Sherrier DJ, Stevens TJ, et al. Prediction of glycosylphosphatidylinositol-anchored proteins in Arabidopsis. A genomic analysis. Plant Physiol. 2002;129(2):486–99.
46. Schmitt AP, McEntee K. Msn2p, a zinc finger DNA-binding protein, is the transcriptional activator of the multistress response in *Saccharomyces cerevisiae*. Proc. Natl. Acad. Sci. U. S. A. 1996;93(12): 5777-82.
47. Raghunath A, Sundarraj K, Nagarajan R, et al. Antioxidant response elements: discovery, classes, regulation and potential applications. Redox Biol. 2018;17:297–314.
48. Liu Y, Ji X, Nie X, et al. Arabidopsis AtbHLH112 regulates the expression of genes involved in abiotic stress tolerance by binding to their E-box and GCG-box motifs. New Phytol. 2015;207(3):692–709.

## Publisher's note